Taylor expansions and Padé approximants for cumulants of conserved charge fluctuations at nonvanishing chemical potentials

D. Bollweg,[1] J. Goswami,[2] O. Kaczmarek,[2] F. Karsch,[2] Swagato Mukherjee,[3] P. Petreczky,[3] C. Schmidt,[2] and P. Scior[3]

(HotQCD Collaboration)

[1]*Physics Department, Columbia University, New York, New York 10027, USA*
[2]*Fakultät für Physik, Universität Bielefeld, D-33615 Bielefeld, Germany*
[3]*Physics Department, Brookhaven National Laboratory, Upton, New York 11973, USA*

(Received 25 February 2022; accepted 1 April 2022; published 28 April 2022)

Using high statistics datasets generated in $(2+1)$-flavor QCD calculations at finite temperature, we present results for low-order cumulants of net-baryon-number fluctuations at nonzero values of the baryon chemical potential. We calculate Taylor expansions for the pressure (zeroth-order cumulant), the net-baryon-number density (first-order cumulant), and the variance of the distribution on net-baryon-number fluctuations (second-order cumulant). We obtain series expansions from an eighth-order expansion of the pressure and compare these to diagonal Padé approximants. This allows us to estimate the range of values for the baryon chemical potential in which these expansions are reliable. We find $\mu_B/T \leq 2.5$, 2.0, and 1.5 for the zeroth-, first-, and second-order cumulants, respectively. We, furthermore, construct estimators for the radius of convergence of the Taylor series of the pressure. In the vicinity of the pseudocritical temperature $T_{pc} \simeq 156.5$ MeV, we find $\mu_B/T \gtrsim 2.9$ at vanishing strangeness chemical potential and somewhat larger values for strangeness neutral matter. These estimates are temperature dependent and range from $\mu_B/T \gtrsim 2.2$ at $T = 135$ MeV to $\mu_B/T \gtrsim 3.2$ at $T = 165$ MeV. The estimated radius of convergences is the same for any higher-order cumulant.

DOI: 10.1103/PhysRevD.105.074511

I. INTRODUCTION

While we gained a lot of information on the thermodynamics of strong interaction matter through numerical calculations in the framework of lattice regularized quantum chromodynamics (QCD) at finite temperature, the extension to nonvanishing values of conserved charge densities, i.e., net baryon number (B), electric charge (Q), and strangeness (S), is difficult due to the lack of appropriate numerical techniques. The currently most actively pursued approaches to QCD at nonzero temperature and nonzero conserved charge densities are based on the application of Taylor series expansions in terms of conserved charge chemical potentials, $\vec{\mu} = (\mu_B, \mu_Q, \mu_S)$ [1,2], or direct simulations at nonzero imaginary chemical potentials [3,4] (for recent reviews, see, e.g., [5–7]). While the former approach has to deal with the range of validity of series expansions arising from a finite radius of convergence of such expansions and truncation errors arising from the limited knowledge on the number of expansion parameters [8], the latter requires analytic continuation to physical, real values of the chemical potential and, thus, is limited by the *Ansatz* used for analytic continuation of thermodynamic observables [9,10], which in practice also is limited by the statistical accuracy with which parameters of such an analytic continuation can be constrained.

Recently, much effort has been put into a better understanding of the analytic structure of the QCD partition function as a function of complex-valued chemical potentials. This is important for our ability to generate suitable *Ansätze* for the analytic continuation of calculations performed with imaginary values of the chemical potentials as well as for choosing appropriate resummation schemes that allow us to extend results obtained in Taylor series beyond the radius of convergence of such expansions. Poles of the logarithm of the QCD partition function in the complex chemical potential plane might be of simple thermal origin, arising, e.g., from the analytic structure of Fermi or Bose distribution functions [11], or stem from universal critical behavior, known as Lee-Yang and Lee-Yang edge singularities [12–15]. Studies of Lee-Yang zeros and

singularities have a long history in QCD; recent studies include, e.g., Refs. [16–18]. The scaling of the Lee-Yang edge singularities and its influence on the QCD phase transition was considered only recently [14,19–22].

We will focus here on the analysis of the Taylor series expansion of the partition function of $(2+1)$-flavor QCD and discuss the resummation of such series using Padé approximants. The range of validity of Taylor expansions using cumulants calculated at physical values of the quark masses is limited by singularities of the logarithm of the QCD partition function, i.e., the pressure, that occur for complex-valued $\vec{\mu}$. These singularities may either occur for real values of $\vec{\mu}$ or in the complex plane, e.g., where $\mathrm{Im}(\mu_B) \neq 0$. Only poles on the real $\vec{\mu}$ axis correspond to phase transitions in QCD. As recent studies of $(2+1)$-flavor QCD with lighter than physical quark masses have shown that the chiral phase transition temperature is at $T_c = 132^{+3}_{-6}$ MeV [23] and as this is expected to set an upper bound on the location of a possible critical point at nonzero values of the baryon chemical potential [24], we expect to find only complex poles for the analytically continued pressure in $(2+1)$-flavor QCD at temperatures above $T \simeq 135$ MeV. Such singularities will limit the radius of convergence for the Taylor series, which has been estimated ever since the first applications of the Taylor expansion approach in lattice QCD calculations [1,2,17].

The singularities in QCD partition functions in the complex μ_B plane also have an impact on the range of applicability of series expansions performed at real values of the chemical potentials. Limitations for the determination of the searched-for critical point in QCD, arising from a finite radius of convergence of Taylor expansions, can, however, be circumvented by using appropriate resummation schemes for the Taylor series [11,18,25–29]. Using Padé approximants is one way to gain information on the analytic structure of the QCD partition function. They allow one to explore, e.g., the pressure of QCD beyond the limit set by a finite radius of convergence of Taylor series [8,21,22,26,30].

Results for Taylor expansion coefficients, i.e., the cumulants χ^{BQS}_{ijk}, in $(2+1)$-flavor QCD up to eighth order, i.e., for all $0 < (i+j+k) \leq 8$, get improved steadily by the HotQCD Collaboration [31–33] in calculations with the highly improved staggered quark (HISQ) action [34]. These expansion coefficients have been used for a determination of the line of pseudocritical temperatures $T_{pc}(\mu_B)$ [31] and in an analysis of high-order cumulants at nonvanishing values of the chemical potentials [32]. The datasets used in these calculations have been extended by adding calculations at a lower temperature, $T \simeq 125$ MeV, for lattices with temporal extent $N_\tau = 8$, and more statistics has been added on lattices with temporal extent $N_\tau = 12$ and 16. Based on these updated datasets, we presented in Ref. [33] an analysis of first- and second-order cumulants at vanishing values of the chemical potentials. Using in addition the results for higher-order cumulants, we present here an analysis of the low-order cumulants at nonvanishing values of the chemical potentials. The datasets that are now available for Taylor coefficients calculated with the HISQ action contain more than a factor of 10 higher statistics on lattices with temporal extent $N_\tau = 8$ and a factor of 20 higher statistics for $N_\tau = 12$ than used previously in studies at nonzero $\vec{\mu}$. This allows a careful analysis of the reliability range of such expansions, on the one hand, and an estimate of the radius of convergence of the Taylor series, on the other hand.

Aside from a systematic discussion of convergence properties of the Taylor series and their improvement through resummation of the series, applying techniques commonly used for other statistical systems, e.g., Padé approximations, the analysis of low-order cumulants also provides the basis for a new, highly improved, analysis of the QCD equation of state of $(2+1)$-flavor QCD at nonvanishing chemical potentials. We provide here results on the pressure and net-baryon-number density and leave the analysis of other bulk thermodynamic observables to a forthcoming publication.

This paper is organized as follows. In Sec. II, we present our results on Taylor expansions for the pressure of $(2+1)$-flavor QCD, the net-baryon-number density, and the second-order cumulant of net-baryon-number fluctuations, involving cumulants of up to eighth order. In Sec. III, we construct Padé approximants for these Taylor series and discuss information on the location of poles closest to the origin that give estimators for the radius of convergence of the Taylor series. Section IV presents a comparison of Taylor series and Padé approximants that allows us to estimate the range of chemical potentials in which current series expansions, that can be constructed by using up to eighth-order cumulants only, provide reliable results. Finally, we give our conclusions in Sec. V. In three Appendixes, we present (Appendix A) an explicit expression for the eighth-order Taylor expansion coefficient of the pressure, (Appendix B) additional expansion coefficients needed for the Taylor series of the second-order cumulant of net-baryon-number fluctuations in strangeness neutral, isospin symmetric systems, and (Appendix C) some details on poles of the diagonal [4,4] Padé for the pressure in $(2+1)$-flavor QCD.

II. TAYLOR EXPANSIONS OF LOW-ORDER CUMULANTS AND THE EQUATION OF STATE

A. Computational setup for Taylor expansion in (2+1)-flavor QCD

The framework for our calculations with the HISQ [34] discretization scheme for $(2+1)$-flavor QCD with a physical strange quark mass and two degenerate, physical light quark masses is well established and has been used by

us in several studies of higher-order cumulants of conserved charge fluctuations and correlations. The specific setup used in our current study has been described in Ref. [32]. The framework for Taylor series expansions for strangeness neutral systems with a fixed ratio of net electric charge to net baryon number has been given up to sixth order in Ref. [35]. It has been extended in Ref. [32] by providing the necessary expansion coefficients for calculations involving up to eighth-order cumulants. In that publication, the eighth-order expansion coefficient of the pressure in strangeness neutral systems was not included. In this work, we present an explicit expression for it in Appendix A.

B. Taylor expansion coefficients up to and including $\mathcal{O}(\mu_B^8)$

We consider thermodynamic quantities, in particular, low-order cumulants of conserved charge fluctuations, derived from Taylor expansions for the pressure of $(2+1)$-flavor QCD:

$$\frac{P}{T^4} = \frac{1}{VT^3} \ln \mathcal{Z}(T,V,\vec{\mu}) = \sum_{i,j,k=0}^{\infty} \frac{\chi_{ijk}^{BQS}}{i!j!k!} \hat{\mu}_B^i \hat{\mu}_Q^j \hat{\mu}_S^k, \quad (1)$$

with $\hat{\mu}_X \equiv \mu_X/T$ and arbitrary natural numbers i, j, and k. The expansion coefficients $\frac{\chi_{ijk}^{BQS}}{i!j!k!}$ are derivatives of P/T^4 with respect to the associated chemical potentials, $\vec{\mu} = (\mu_B, \mu_Q, \mu_S)$, evaluated at $\vec{\mu} = \vec{0}$:

$$\chi_{ijk}^{BQS} = \frac{1}{VT^3} \frac{\partial \ln \mathcal{Z}(T,V,\vec{\mu})}{\partial \hat{\mu}_B^i \partial \hat{\mu}_Q^j \partial \hat{\mu}_S^k}\bigg|_{\vec{\mu}=0}, \quad i+j+k \text{ even}. \quad (2)$$

Aside from the Taylor expansion of the pressure, we will focus here on the analysis of Taylor series for the first- and second-order cumulants of net-baryon-number fluctuations:

$$n_B = \frac{\partial P/T^4}{\partial \hat{\mu}_B}, \quad (3)$$

$$\chi_2^B = \frac{\partial^2 P/T^4}{\partial \hat{\mu}_B^2}. \quad (4)$$

For these observables we will introduce constraints on the electric charge and strangeness chemical potentials [32,35]:

$$\begin{aligned} \hat{\mu}_Q(T,\mu_B) &= q_1(T)\hat{\mu}_B + q_3(T)\hat{\mu}_B^3 + q_5(T)\hat{\mu}_B^5 + \cdots, \\ \hat{\mu}_S(T,\mu_B) &= s_1(T)\hat{\mu}_B + s_3(T)\hat{\mu}_B^3 + s_5(T)\hat{\mu}_B^5 + \cdots \end{aligned} \quad (5)$$

that enforce strangeness neutrality ($n_S = 0$) and a fixed ratio $n_Q/n_B = r$. Here, the case $r = 0.5$ refers to an isospin symmetric medium, which is realized for $\mu_Q = 0$. The case $r = 0.4$ corresponds to the situation met in heavy ion collision experiments. Explicit expressions for the expansion coefficients q_i and s_i with $i = 1, 3, 5$ are given in Ref. [35]; the coefficients q_7 and s_7 are given in Ref. [32]. With these constraints, we arrive at Taylor series in terms of the baryon chemical potential only:

$$\chi_n^B(T,\hat{\mu}_B) = \sum_k \frac{\bar{\chi}_n^{B,k}(T)}{k!} \hat{\mu}_B^k, \quad (6)$$

where $n = 0$ corresponds to the Taylor series for the $\hat{\mu}_B$-dependent part of the pressure, $n = 1$ gives the net-baryon-number density, and $n > 2$ gives higher-order cumulants of net-baryon-number fluctuations:

$$\chi_0^B(T,\hat{\mu}_B) \equiv \frac{P(T,\mu_B) - P(T,0)}{T^4} = \sum_{k=1}^{\infty} P_{2k}(T)\hat{\mu}_B^{2k}, \quad (7)$$

$$\chi_1^B(T,\hat{\mu}_B) \equiv \frac{n_B(T,\mu_B)}{T^3} = \sum_{k=1}^{\infty} N_{2k-1}^B(T)\hat{\mu}_B^{2k-1}, \quad (8)$$

$$\chi_2^B(T,\mu_B) = \sum_{k=0}^{\infty} \tilde{\chi}_2^{B,k}(T)\hat{\mu}_B^{2k}, \quad (9)$$

with $P_{2k} \equiv \bar{\chi}_0^{B,2k}/(2k)!$ and $N_{2k-1}^B = \bar{\chi}_1^{B,2k-1}/(2k-1)!$. The expansion coefficients $\bar{\chi}_n^{B,k}$ are simply related to the expansion coefficients $\tilde{\chi}_n^{B,k}$ defined in Ref. [32]:

$$\tilde{\chi}_n^{B,k} \equiv \frac{\bar{\chi}_n^{B,k}}{k!}. \quad (10)$$

For convenience, we use here $\bar{\chi}_n^{B,k}$ rather than $\tilde{\chi}_n^{B,k}$, as this emphasizes the close relation of the constraint expansion coefficients to the standard cumulants of net-baryon-number fluctuations χ_k^B which equal $\bar{\chi}_n^{B,k}$ in the case $\mu_Q = \mu_S = 0$. Explicit expressions for $\bar{\chi}_n^{B,k}$ are given in Appendix A in Ref. [32] for $k \leq 7$. For $k = 8$, we give the expansion coefficient $\bar{\chi}_n^{B,8}$ here in Appendix A. We also note that, in the case $\mu_Q = \mu_S = 0$ as well as in the isospin symmetric case $r = 1/2$, the expansion coefficients for the pressure and number density series are closely related:

$$N_{2k-1}^B(T) = 2kP_{2k}(T). \quad (11)$$

In fact, in the case $\mu_Q = \mu_S = 0$ the expansion coefficients of all higher-order cumulants are simply related to those of the pressure series: $\bar{\chi}_n^{B,k} = \frac{(k+n)!}{k!}\bar{\chi}_0^{B,k+n}$. The expansion coefficients shown in Fig. 1, thus, are sufficient to construct the expansions for P/T^4 ($n = 0$), n_B/T^3 ($n = 1$), and χ_2^B ($n = 2$). In the strangeness neutral case, $\mu_Q = 0$, $n_S = 0$, the above relation holds only for $n = 1$. We, thus, still need to give results for the expansion coefficients of $\bar{\chi}_2^{B,k}$ with

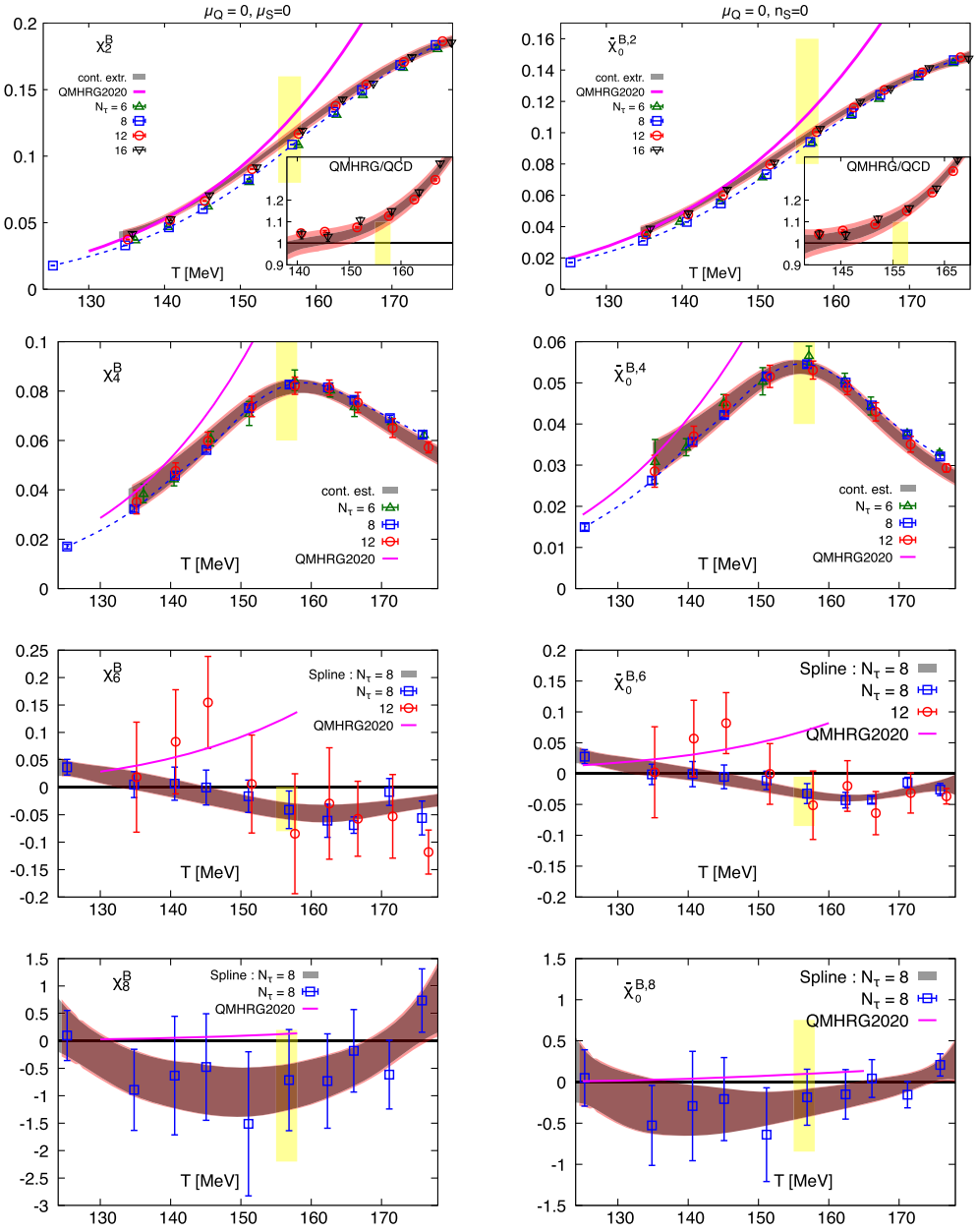

FIG. 1. The nth-order cumulants $\bar{\chi}_0^{B,n}$, contributing to the Taylor series of the pressure of $(2+1)$-flavor QCD as a function of $\hat{\mu}_B = \mu_B/T$ versus temperature. Shown are the expansion coefficients for the cases of (i) $\mu_Q = \mu_S = 0$ (left column) and (ii) $\mu_Q = 0$, $n_S = 0$ (right column), respectively. In both cases, the actual nth-order expansion coefficients in the Taylor series are obtained with these cumulants as $\bar{\chi}_0^{B,n}/n!$. Yellow bands show the location of the pseudocritical temperature $T_{pc}(0) = 156.5(1.5)$ MeV [31].

$k = 2,\ 4,\ 6$. We show these expansion coefficients in Appendix B. As expected, the qualitative features of the temperature dependence of $\bar{\chi}_2^{B,k}$ in the $n_S = 0$ and $\mu_S = 0$ cases are similar; i.e., they behave like χ_{k+2}^B.

In Fig. 1, we show results for $\bar{\chi}_0^{B,2k}$ for the two different cases considered throughout this paper; i.e., we work in the isospin symmetric case, corresponding to $\mu_Q = 0$, and consider for the strangeness sector (i) the case $\mu_S = 0$ (left) and (ii) the strangeness neutral case $n_S = 0$ (right), respectively. Continuum extrapolated results for the leading-order expansion coefficient of the pressure series, $\bar{\chi}_0^{B,2}$, are shown in the two panels on the top in Fig. 1. They are based on datasets generated on lattices with temporal extent $N_\tau = 6$, 8, 12, and 16. Results for the case $\mu_Q = \mu_S = 0$ at $T \gtrsim 135$ MeV had been shown already in Ref. [33]; we added here our results at $T = 125$ MeV obtained on lattices with temporal extend $N_\tau = 8$, which have not been used in the continuum extrapolations. The insets given in these figures for χ_2^B (left) as well as $\bar{\chi}_0^{B,2}$ (right) show comparisons with the same cumulants

calculated in a hadron resonance gas (HRG) model describing the thermodynamics of noninteracting, pointlike hadrons.[1] This calculation uses the hadron spectrum compiled in the QMHRG2020 list [33].

For the $\mathcal{O}(\hat{\mu}_B^4)$ expansion coefficients, we show in Fig. 1 continuum extrapolations based on $N_\tau = 6$, 8, and 12 datasets. For the higher-order expansion coefficients, we use only results from our high statistics calculations on lattices with temporal extent $N_\tau = 8$, where more than 1.5 million gauge field configurations[2] have been generated at each temperature value. Results for larger N_τ are consistent with these results but have significantly larger statistical errors. However, as can be seen from the lower-order expansion coefficients, cutoff effects are generally small for expansion coefficients at nonzero values of $\hat{\mu}_B$. The interpolating curves for the $\mathcal{O}(\mu_B^6)$ and $\mathcal{O}(\mu_B^8)$ expansion coefficients shown in Fig. 1 are cubic spline interpolations.

C. Cumulants and the equation of state at nonzero μ_B

From the temperature dependence of the $\mathcal{O}(\hat{\mu}_B^2)$ expansion coefficient of the pressure shown in Fig. 1, it is apparent that deviations from the thermodynamics of a noninteracting HRG reach about 20% at the pseudocritical temperature of $(2+1)$-flavor QCD, $T_{pc}(0) = 156.5(1.5)$ MeV [31], and rapidly become larger at higher temperatures. Below T_{pc}, the leading-order expansion coefficient agrees quite well with HRG model calculations [33]. As can be seen also in Fig. 1, already the $\mathcal{O}(\hat{\mu}_B^4)$ Taylor coefficient deviates from HRG model results more strongly than the $\mathcal{O}(\hat{\mu}_B^2)$ expansion coefficient. For all temperatures in the range 135 MeV $\leq T \leq$ 165 MeV, the sixth- and eighth-order expansion coefficients are negative, in contrast to the noninteracting HRG expansion coefficients, which are all positive. Even at low temperatures, we, thus, expect to find that deviations from HRG model calculations increase with increasing values of the baryon chemical potential.

Compared to our earlier analysis of the QCD equation of state, presented in Ref. [35], the new results for the expansion coefficients shown in Fig. 1 are based on 10 times higher statistics for $N_\tau = 8$ and 12 and include also data on lattices with temporal extent $N_\tau = 16$. This allows us to determine also the contribution from eighth-order expansion coefficients to Taylor series of various thermodynamic observables. The highly improved statistics results in a huge improvement of the current calculation over that published previously [35]. We update in Fig. 2 our results for the pressure and the net-baryon-number density calculated in sixth and fifth orders of the Taylor expansion, respectively. Results are shown as a function of temperature for the case $\mu_Q = \mu_S = 0$ using the continuum extrapolated data for χ_2^B and χ_4^B, as well as the spline interpolated data for χ_6^B, obtained on lattices with temporal extent $N_\tau = 8$. Obviously, the "wiggly" structure seen in the old calculations for $\mathcal{O}(\hat{\mu}_B^6)$ expansions at $\hat{\mu}_B = 2.5$ [35] is smoothed out in our new high statistics analysis, and the $\mathcal{O}(\hat{\mu}_B^6)$ results agree well with $\mathcal{O}(\hat{\mu}_B^4)$ expansions in the entire temperature range.

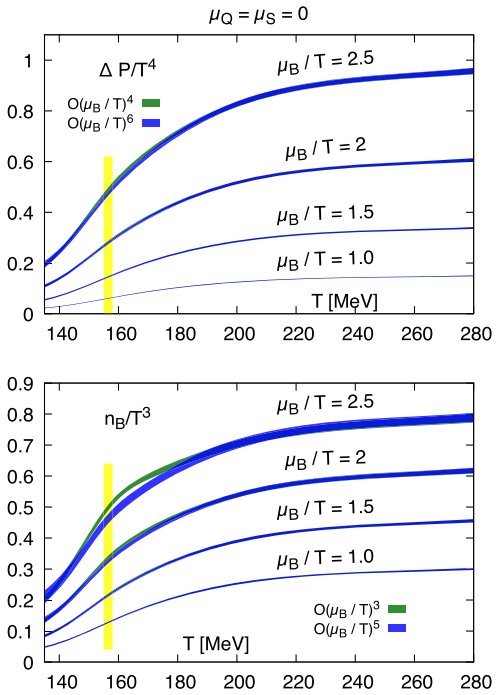

FIG. 2. Fourth- and sixth-order Taylor series results for the pressure and corresponding third- and fifth-order expansion results for the net-baryon-number density as a function of temperature for the case $\mu_Q = \mu_S = 0$.

On the basis of a sixth-order Taylor expansion, we, thus, have no indications for a radius of convergence being smaller than $\hat{\mu}_B = 2.5$, nor do we have indications for a poor convergence of the Taylor expansions of P/T^4 and n_B/T^3, respectively. This will change when discussing the eighth-order contribution to the Taylor series. We stress, however, already here that we need to distinguish between the radius of convergence of the Taylor series, which is the same for all observables determined as derivatives of P/T^4 with respect to $\hat{\mu}_B$, and the rate of convergence of expansions for these observables to their asymptotic values, which will be slower with increasing order of the derivatives.

[1]Throughout this work, we use a model based on noninteracting, pointlike hadrons listed in the QMHRG2020 list [33] as the HRG model reference system. Such models have been improved by incorporating interactions as described by the S matrix [36] or more phenomenological through the use of finite volume for baryons [37].

[2]These datasets have been generated using a rational hybrid Monte Carlo algorithm (RHMC) [38,39]. They contain gauge field configurations that have been stored after ten subsequent RHMC time units. The actual code package used for our calculations is described in Ref. [40].

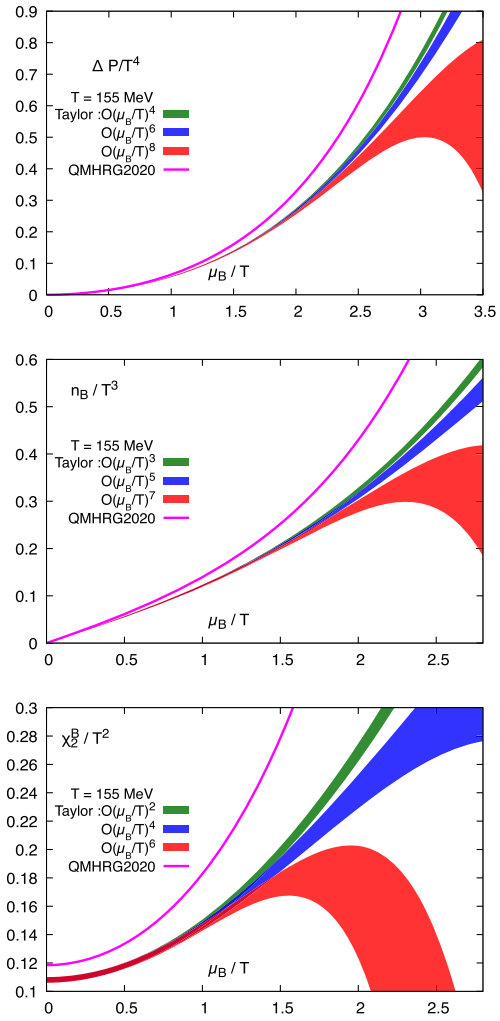

FIG. 3. The pressure (top), net-baryon-number density (middle), and net-baryon-number fluctuations (bottom) versus $\hat{\mu}_B$ at $T = 155$ MeV.

Taking also into account the contribution from eighth-order Taylor expansion coefficients of the pressure, we show in Fig. 3 results for the $\hat{\mu}_B$ dependence of the pressure, net-baryon-number density, and the second-order cumulant of net-baryon-number fluctuations. Shown are results obtained by using different orders of the Taylor expansion at a fixed value of the temperature in the vicinity of T_{pc}, i.e., $T = 155$ MeV, for the case $\mu_Q = \mu_S = 0$. As can be seen, deviations from QMHRG2020 increase with increasing $\hat{\mu}_B$, and these deviations are larger for higher-order cumulants. It also is apparent from this figure that the rate of convergence of the expansions for higher-order cumulants slows down. Being limited to a certain order in the expansion, thus, allows us to give reliable results for higher-order cumulants only in a smaller $\hat{\mu}_B$ range, although the expansions for all cumulants have the same radius of convergence. We will give a more quantitative discussion of the $\hat{\mu}_B$ range, in which the current Taylor expansions for different cumulants are expected to give reliable results, in Sec. IV.

In Fig. 4, we show the $\hat{\mu}_B$-dependent contribution to the pressure as a function of temperature for some values of $\hat{\mu}_B$, i.e., for $\hat{\mu}_B = 1.0$, 1.5, 2.0, and 2.5, and for the net-baryon-number density for $\hat{\mu}_B = 1.0$, 1.5, 2.0. In all cases, we show results obtained in different orders of the Taylor series expansion. For these values of the baryon chemical potential, the $\mathcal{O}(\hat{\mu}_B^8)$ Taylor series for the pressure agrees well with the lower-order results. For n_B/T^3, we do not show results from an $\mathcal{O}(\hat{\mu}_B^8)$ at $\hat{\mu}_B = 2.5$, as it is apparent from Fig. 3 that higher-order expansion coefficients will be needed to obtain reliable results for the pressure at that large value of $\hat{\mu}_B$.

In the entire temperature range analyzed by us, the Taylor series for pressure converges well for $0 \leq \hat{\mu}_B \leq 2.5$. For the number density, this can be stated at present only for the range $0 \leq \hat{\mu}_B \leq 2.0$, although that may turn out to be somewhat larger once the statistical accuracy in calculations of eighth-order expansion coefficients is increased. Nonetheless, based on the analysis of eighth-order Taylor expansions of the pressure, we have no hint for a radius of convergence smaller than $\hat{\mu}_B \sim 2.5$ that would limit the applicability of Taylor expansions at temperatures $T \gtrsim 125$ MeV.

III. RADIUS OF CONVERGENCE AND PADÉ APPROXIMATIONS

In general, the radius of convergence of the Taylor series for a function

$$f(x) = \sum_n^\infty c_n x^n \tag{12}$$

is given by the location of a singularity of f in the complex x plane that is closest to the origin. Of course, rigorous statements on the radius of convergence of a Taylor series can be made only by analyzing the asymptotic behavior of the expansion coefficients in the limit $n \to \infty$. Having at hand only a few expansion coefficients of the Taylor series for the pressure in QCD, we naturally can obtain estimators only for the radius of convergence and extract some information on the analytic structure of thermodynamic functions in the plane of complex chemical potentials.

We are dealing with Taylor series in terms of $\hat{\mu}_B$ for which only every second expansion coefficient is nonzero, e.g., the pressure series which has nonvanishing expansion coefficients $\bar{\chi}_0^{B,n}$ only for even n. The simplest estimator $r_{c,n}$ for the radius of convergence $r_c = \lim_{n\to\infty} r_{c,n}$ is obtained from subsequent, nonvanishing expansion coefficients. We define $r_{c,n} = \sqrt{|A_n|}$, with

$$A_n = \frac{c_n}{c_{n+2}}, \qquad n \text{ even}. \tag{13}$$

Another frequently used estimator, with improved convergence properties, has been introduced by Mercer and Roberts [41], $r_{c,n}^{MR} = |A_n^{MR}|^{1/4}$, with

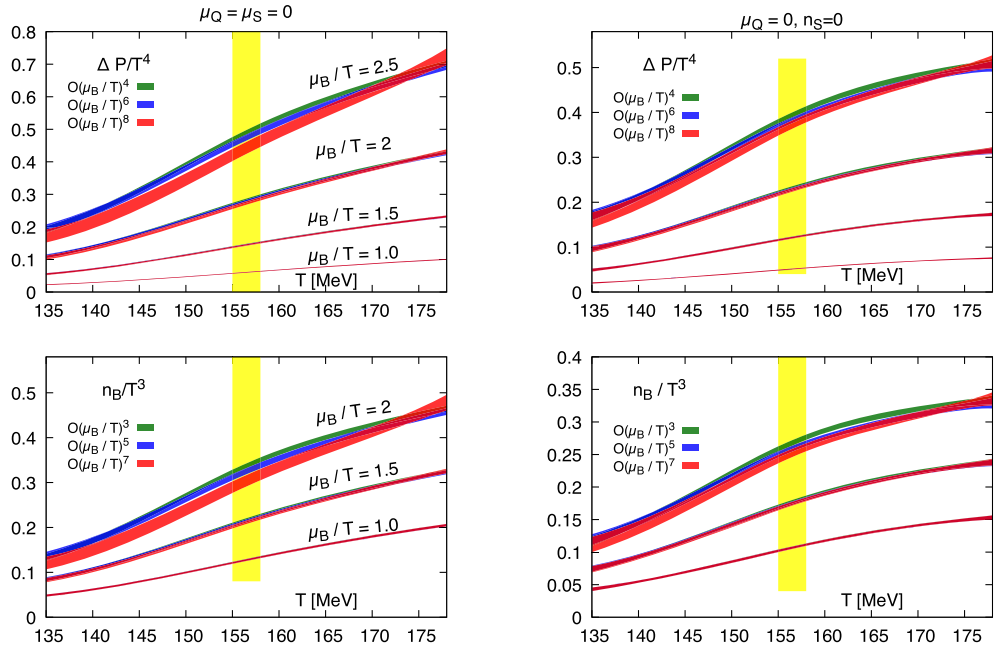

FIG. 4. Pressure (top) and net-baryon-number density (bottom) versus temperature for several values of the baryon chemical potential. Figures on the left correspond to the case $\mu_Q = \mu_S = 0$ and on the right to the strangeness neutral, isospin symmetric case. The Taylor expansions are based on the continuum and spline interpolated data shown in Fig. 1.

$$A_n^{MR} = \frac{c_{n+2}c_{n-2} - c_n^2}{c_{n+4}c_n - c_{n+2}^2}, \qquad n \text{ even}. \tag{14}$$

The estimators based on the ratios A_n and A_n^{MR} are related to poles of $[n,2]$ and $[n,4]$ Padé approximants for the series expansion of $f(x)$. We, thus, will consider the structure of such Padé approximants in the following.

When constructing Padé approximants for the pressure series of $(2+1)$-flavor QCD, we take advantage of the fact that the two leading expansion coefficients of the pressure, $P_{2k} = \bar{\chi}_0^{B,2k}/(2k)!$, $k = 1, 2$, are strictly positive. We, thus, rescale the pressure by a factor P_4/P_2^2 and redefine the expansion parameter as

$$\bar{x} = \sqrt{\frac{P_4}{P_2}}\hat{\mu}_B \equiv \sqrt{\frac{\bar{\chi}_0^{B,4}}{12\bar{\chi}_0^{B,2}}}\hat{\mu}_B. \tag{15}$$

This allows us to rewrite the expansion of the pressure in terms of expansion coefficients

$$c_{2k,2} = \frac{P_{2k}}{P_2}\left(\frac{P_2}{P_4}\right)^{k-1}, \tag{16}$$

which gives $c_{2,2} = c_{4,2} = 1$. Therefore, for $\mu_Q = \mu_S = 0$ as well as for the strangeness neutral case, the analytic structure of the QCD pressure, that one can deduce from an eighth-order Taylor series in QCD, entirely depends on two expansion parameters:

$$c_{6,2} = \frac{P_6 P_2}{P_4^2} = \frac{2}{5}\frac{\bar{\chi}_6^B \bar{\chi}_2^B}{(\bar{\chi}_4^B)^2}, \tag{17}$$

$$c_{8,2} = \frac{P_8 P_2^2}{P_4^3} = \frac{3}{35}\frac{\bar{\chi}_8^B (\bar{\chi}_2^B)^2}{(\bar{\chi}_4^B)^3}. \tag{18}$$

With this, we obtain

$$\frac{(\Delta P(T,\mu_B)/T^4)P_4}{P_2^2} = \sum_{k=1}^{\infty} c_{2k,2}\bar{x}^{2k} = \bar{x}^2 + \bar{x}^4 + c_{6,2}\bar{x}^6 + c_{8,2}\bar{x}^8 + \cdots, \tag{19}$$

with $\Delta P(T,\mu_B) = P(T,\mu_B) - P(T,0)$.

The two diagonal Padé approximants that can be constructed from our eighth-order series for the pressure are given by

$$P[2,2] = \frac{\bar{x}^2}{1-\bar{x}^2}, \tag{20}$$

$$P[4,4] = \frac{(1-c_{6,2})\bar{x}^2 + (1-2c_{6,2}+c_{8,2})\bar{x}^4}{(1-c_{6,2}) + (c_{8,2}-c_{6,2})\bar{x}^2 + (c_{6,2}^2 - c_{8,2})\bar{x}^4}. \tag{21}$$

The [2, 2] Padé has a pole on the real axis for $\bar{x}^2 = 1$, i.e., for $\mu_{B,c} \equiv r_{c,2} = \sqrt{12\bar{\chi}_2^B/\bar{\chi}_4^B}$, which is the standard ratio estimator for the radius of convergence. The [4, 4] Padé has four poles which come in two pairs, corresponding to zeros

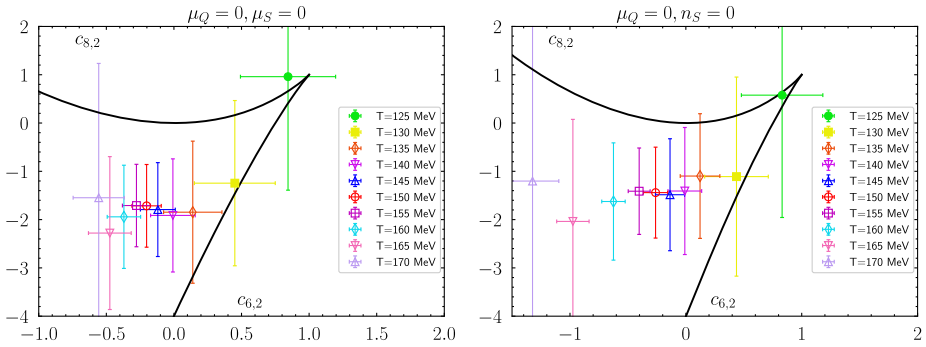

FIG. 5. The expansion coefficients $c_{8,2}$ versus $c_{6,2}$ on lattices with temporal extent $N_\tau = 8$ in the entire temperature range 125 MeV $< T <$ 175 MeV covered in our calculations. The area bounded by the two black lines indicates the region in parameter space, in which all poles of the [4, 4] Padé are complex. The left-hand figure corresponds to the case $\mu_Q = \mu_S = 0$, and the right-hand figure is for the strangeness neutral, isospin symmetric case.

of the polynomial in the denominator of Eq. (21) which is quadratic in $z \equiv \bar{x}^2$. The two zeros in z are given by

$$z^{\pm} = \frac{c_{8,2} - c_{6,2} \pm \sqrt{(c_{8,2} - c^{+}_{8,2})(c_{8,2} - c^{-}_{8,2})}}{2(c_{8,2} - c^{2}_{6,2})}, \qquad (22)$$

with

$$c^{\pm}_{8,2} = -2 + 3c_{6,2} \pm 2(1 - c_{6,2})^{3/2}. \qquad (23)$$

It is easy to see that the argument of the square root appearing in Eq. (22) is positive for $c_{6,2} > 1$. Complex zeros with $\mathrm{Re}(\hat{\mu}_B) \neq 0$ thus exist only for

$$\text{(i) } c_{6,2} < 1 \quad \text{and} \quad c^{-}_{8,2} < c_{8,2} < c^{+}_{8,2}. \qquad (24)$$

Outside this region, the zeros $z^{\pm}$ are real and, thus, correspond to pairs of real poles in terms of $\hat{\mu}_B$ if $z^{\pm} > 0$ and purely imaginary poles if $z^{\pm} < 0$. In fact, as we show in Appendix C, there is a small region in parameter space $(c_{6,2}, c_{8,2})$, close to $c^{+}_{8,2}$ in which $z^{+} < 0$ and $z^{-} < 0$,

$$\text{(ii) } c_{6,2} < 0 \quad \text{and} \quad c^{+}_{8,2} < c_{8,2} < c^{2}_{6,2}. \qquad (25)$$

This leads to two pairs of purely imaginary poles in $\hat{\mu}_B$. Everywhere else in parameter space, at least one pair of real zeros exists, which, however, not always is the pair of zeros closest to the origin (see Appendix C).

In order to get further information on the poles of the [4, 4] Padé approximant for the pressure and, in particular, deduce conditions for the occurrence of real poles, we show in Fig. 5 results for $c_{8,2}$ versus $c_{6,2}$ obtained in the temperature range[3] 125 MeV $\leq T \leq$ 170 MeV from the spline interpolated $N_\tau = 8$ expansion coefficients, $\bar{\chi}^{B,6}_0$ and $\bar{\chi}^{B,8}_0$, and the continuum extrapolations for $\bar{\chi}^{B,2}_0$ and $\bar{\chi}^{B,4}_0$ shown in Fig. 1. Also shown in this figure are the boundaries for the triangular-shaped region, bounded by $c^{+}_{8,2}$ and $c^{-}_{8,2}$, inside which only complex poles exist for the [4, 4] Padé of the eighth-order Taylor series of the pressure. We show results for the case $\mu_Q = \mu_S = 0$ (left) and $\mu_Q = 0$, $n_S = 0$ (right), respectively.

As can be seen in Fig. 5, despite the currently large errors on the location of the poles, it is well established that the poles occur in the complex $\hat{\mu}_B$ plane for all temperatures 135 MeV $\leq T \leq$ 165 MeV. Within our current statistical errors, we cannot rule out that pairs of real and/or purely imaginary poles will occur at temperatures below $T =$ 135 MeV as well as for temperatures above $T =$ 165 MeV. In fact, this is expected to be the case at low enough temperatures, where one can see in Fig. 1 that $\bar{\chi}^{B,6}_0$ and $\bar{\chi}^{B,8}_0$ become positive at $T \simeq$ 125 MeV, and also at high temperature, where Fig. 1 shows that $\bar{\chi}^{B,6}_0 < 0$ while $\bar{\chi}^{B,8}_0 > 0$ at $T \simeq$ 175 MeV.

At low temperatures, the complex-valued poles leave the area bounded by $c^{\pm}_{8,2}$ in a region of parameter space where $c_{6,2} > 0$ or, correspondingly, $\bar{\chi}^{B,6}_0 > 0$. As discussed and also indicated in the figure shown in Appendix C, for $c_{6,2} > 0$ there is a small region in parameter space above the boundary defined by $c^{+}_{8,2}$ where all poles are strictly real, before entering the region where a pair of real and imaginary poles exists. One can check that for all $0 < c_{6,2} < 1$ the real pole actually is closer to the origin as long as $c^{2}_{6,2} < c_{8,2} < c_{6,2}$. Our results on the temperature dependence of $c^{2}_{6,2}$ and $c^{2}_{8,2}$, thus, suggest that with decreasing temperature a pair of complex poles moves toward the real axis and gives rise to two real poles. With decreasing temperature, one of these real poles moves toward infinity and comes back as an imaginary pole with large magnitude.

In the region where the conditions given in Eq. (24) hold, one has four zeros in terms of $\bar{x}$ corresponding to the

[3]We do not show results for $T =$ 175 MeV, as errors are even larger than those shown for $T =$ 170 MeV.

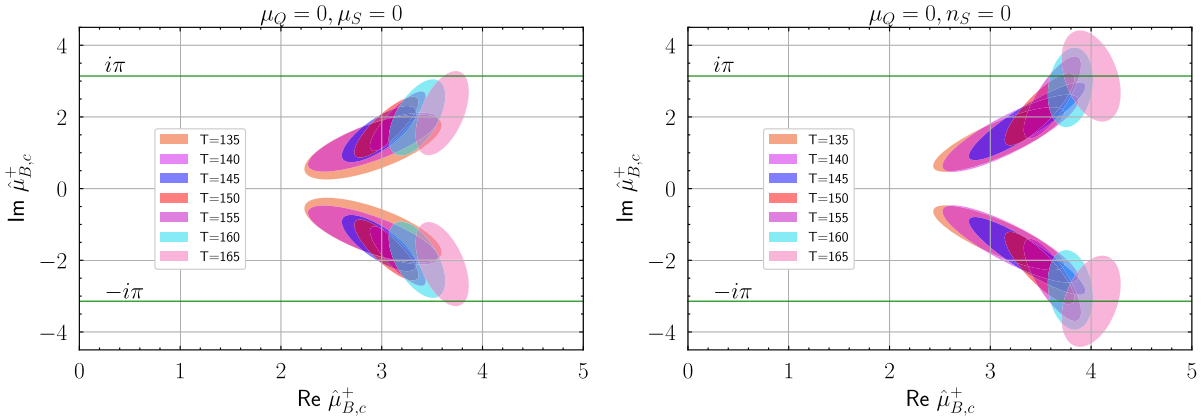

FIG. 6. Location of poles nearest to the origin obtained from the [4, 4] Padé approximants in the complex $\hat{\mu}_B$ plane. Only poles with $\mathrm{Re}(\mu_B) > 0$ are shown. Shown are results for the case $\mu_Q = \mu_S = 0$ (left) and the strangeness neutral, isospin symmetric case (right).

positive and negative roots of $z^{\pm}$. They yield four poles of the [4, 4] Padé in the complex μ_B plane with the non-vanishing imaginary part of $\hat{\mu}_B$. We represent these poles in polar coordinates:

$$\hat{\mu}^{\pm}_{B,c} = \pm r_{c,4} e^{\pm i\Theta_{c,4}}. \tag{26}$$

For temperatures 135 MeV $\leq T \leq$ 165 MeV, the zeros $z^{\pm}$ are complex conjugate to each other. In the $\bar{x}$ plane, the absolute value of the distance of the poles from the origin is then given by

$$|z^+ z^-|^{1/4} = \left| \frac{1 - c_{6,2}}{c_{6,2}^2 - c_{8,2}} \right|^{1/4}, \tag{27}$$

which is the Mercer-Roberts estimator, introduced in Eq. (14), for a series in the rescaled expansion parameter $\bar{x}$. We note that this relation between the Mercer-Roberts estimator and the magnitude of $|z^{\pm}|$ does not hold for the case of purely real or purely imaginary poles of the [4, 4] Padé (see discussion in Appendix C). In these cases, the distances to the origin $|z^+|$ and $|z^-|$ differ from each other.

Using Eqs. (26) and (27), we obtain for $c_{6,2} < 1$ the location of the poles in the complex μ_B plane:

$$r_{c,4} = r_{c,2}|z^+ z^-|^{1/4} = \sqrt{\frac{12\bar{\chi}_0^{B,2}}{\bar{\chi}_0^{B,4}}} \left| \frac{1 - c_{6,2}}{c_{6,2}^2 - c_{8,2}} \right|^{1/4}, \tag{28}$$

$$\Theta_{c,4} = \arccos\left(\frac{c_{6,2} - c_{8,2}}{2\sqrt{(1 - c_{6,2})(c_{6,2}^2 - c_{8,2})}} \right) = \arccos\left(\frac{(c_{6,2} - c_{8,2})\bar{\chi}_0^{B,4}}{24(1 - c_{6,2})\bar{\chi}_0^{B,2}} r_{c,4}^2 \right). \tag{29}$$

Expressing the relation given in Eq. (28) in terms of the cumulants $\bar{\chi}_0^{B,n}$ entering the Taylor series for the pressure [Eq. (7)], we have in the region of complex poles

$$r_{c,4} = \left(\frac{8!}{4!} \right)^{1/4} \left| \frac{30(\bar{\chi}_0^{B,4})^2 - 12\bar{\chi}_0^{B,6}\bar{\chi}_0^{B,2}}{56(\bar{\chi}_0^{B,6})^2 - 30\bar{\chi}_0^{B,8}\bar{\chi}_0^{B,4}} \right|^{1/4}. \tag{30}$$

The positions of the poles in the complex $\hat{\mu}_B$ plane are shown in Fig. 6. Only the two poles in the region $\mathrm{Re}(\hat{\mu}_B) \geq 0$ are shown. With decreasing temperature, the poles move closer to the real axis as $c_{8,2}$ approaches $c_{8,2}^+$, i.e., $\Theta_{c,4} = 0$ for $c_{8,2} = c_{8,2}^+$. Furthermore, it is clear from Eq. (29) that $\Theta_{c,4}$ and $r_{c,4}$ are correlated, which leads to the orientation of the 1σ error ellipse in the complex $\mu_{B,c}$ plane arising from the errors on $c_{6,2}$ and $c_{8,2}$, which are assumed to given by independent Gaussian distributions of the variables $c_{6,2}$ and $c_{8,2}$.

In Fig. 7, we show as symbols and bands, respectively, the distance of poles of the [2, 2] and [4, 4] Padé approximants from the origin as a function of temperature. The bands shown in Fig. 7 have been obtained by using the spline interpolations of $\bar{\chi}_0^{B,6}$ and $\bar{\chi}_0^{B,8}$ on $N_\tau = 8$

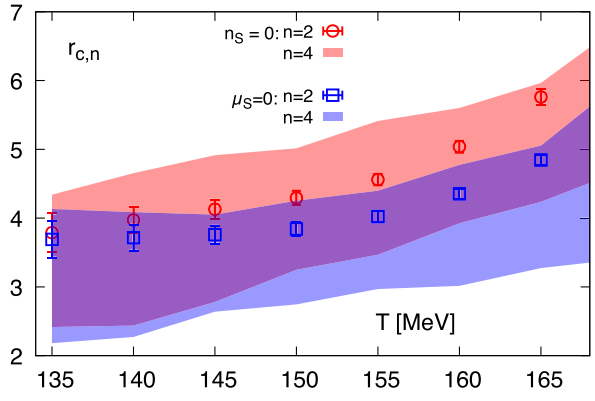

FIG. 7. Magnitude of poles nearest to the origin obtained from the [2, 2] (squares and circles) and [4, 4] (bands) Padé approximants for Taylor expansions at $\mu_Q = \mu_S = 0$ and for strangeness neutral, isospin symmetric media, respectively.

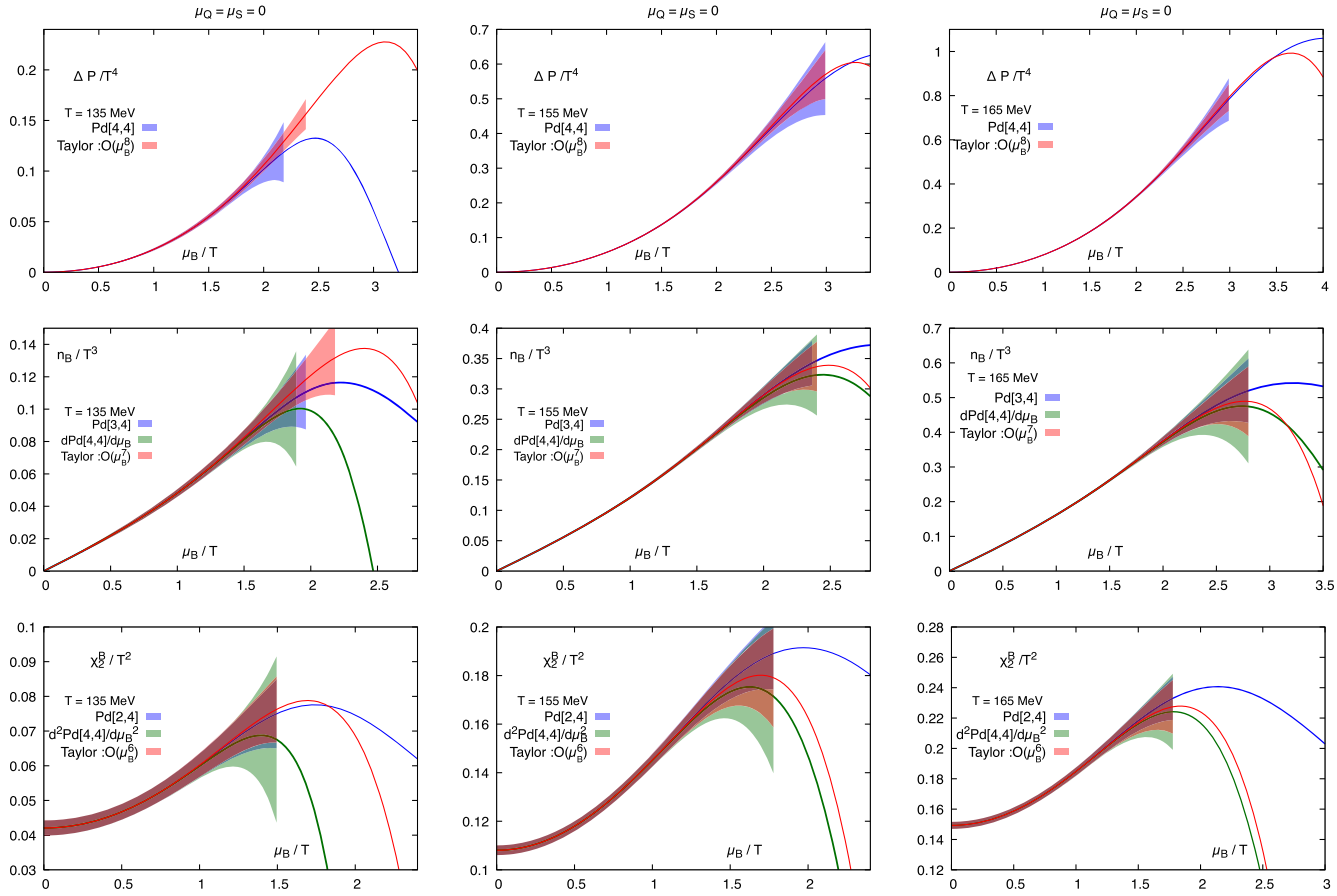

FIG. 8. Comparison of the $[n, 4]$ Padé approximants for the pressure ($n = 4$), the net-baryon-number density ($n = 3$), and the second-order cumulant of net-baryon-number fluctuations ($n = 2$) with corresponding Taylor expansions. Shown are results for $T = 135$ (left), 155 (middle), and 165 MeV (right) versus $\hat{\mu}_B$ for the case $\mu_Q = \mu_S = 0$. Also shown are derivatives of the [4, 4] Padé approximants with respect to $\hat{\mu}_B$ (green bands).

lattices and the continuum extrapolated results for $\bar{\chi}_0^{B,2}$ and $\bar{\chi}_0^{B,4}$, shown in Fig. 1, respectively. As can be seen, the two estimators yield a similar magnitude for $r_{c,2}$ and $r_{c,4}$. Their location in the complex μ_B plane, however, is quite different. While the poles of the [2, 2] Padé are always on the real axis, the poles of the [4, 4] Padé are in the complex plane in the entire interval 135 MeV $\leq T \leq$ 165 MeV.

For 135 MeV $\leq T \leq$ 165 MeV, we find that the poles of the [4, 4] Padé appear at a distance from the origin corresponding to $|\hat{\mu}_B| \gtrsim 2.5$ at $T \simeq 135$ MeV and rise to values larger than $|\hat{\mu}_B| \gtrsim 3$ for $T \gtrsim T_{pc}$. These also are the best estimates for a temperature-dependent bound on the radius of convergence of the Taylor series for the pressure, based on the Mercer-Roberts estimator. The information extracted from the [4, 4] Padé approximants on the location of poles in the analytic function representing the pressure as a function of a complex-valued chemical potential $\hat{\mu}_B$, thus, seems to be consistent with the good convergence properties of the Taylor series itself.

IV. COMPARISON OF PADÉ APPROXIMANTS AND TAYLOR SERIES

In Fig. 8, we compare the $[n, 4]$ Padé approximants for the pressure ($n = 4$), the net-baryon-number density ($n = 3$), and the second-order cumulant of net-baryon-number fluctuations ($n = 2$) with corresponding Taylor expansions that use expansion coefficients $\bar{\chi}_{4-n}^{B,k}$ with $k \leq 8$. We show results obtained at three temperatures in the interval in which our results clearly yield complex-valued poles only, i.e., $T = 135$, 155, and 165 MeV, respectively. As error bands quickly become large for large $\hat{\mu}_B$, we show errors only up to the point where relative errors are less then 15%. In this range of $\hat{\mu}_B$ values, also the Padé approximants and the straightforward Taylor expansions agree quite well.

In the entire temperature interval 135 MeV $\leq T \leq$ 165 MeV, the expansion coefficient $\bar{\chi}_0^{B,8}$ is negative for $\mu_Q = \mu_S = 0$ as well as for $\mu_Q = 0$, $n_S = 0$. It will dominate the expansion at large $\hat{\mu}_B$ and, thus, forces the Taylor expansion of P/T^4 to have a maximum at some value of $\hat{\mu}_B^{\max}$. As the net-baryon-number density is the

derivative of P/T^4 with respect to $\hat{\mu}_B$, it has a maximum below $\hat{\mu}_B^{\max}$ and vanishes at $\hat{\mu}_B^{\max}$. Similarly, the second-order cumulant reaches a maximum at an even smaller value of $\hat{\mu}_B$. As can be seen in Fig. 8, the $[n,4]$ Padé approximants (blue bands), the direct $\hat{\mu}_B$ derivative of the [4, 4] Padé (green bands), and the Taylor expansions (red bands) agree quite well up to values of the chemical potentials close to the respective value of $\hat{\mu}_B^{\max}$, and this maximum arises at larger $\hat{\mu}_B$ as the temperature increases. This is in accordance with the increase of the estimator $\mu_{c,4}^{MR}(T)$ for the magnitude of the Padé poles given in Fig. 7.

Starting with a Taylor series limited to eighth order, obviously the expansions possible for higher-order derivatives become shorter. Correspondingly, the order of an $[n,4]$ Padé used by us becomes smaller. If, however, the Padé approximant used for the original pressure series, i.e., in our case the [4, 4] Padé approximant, provides a good approximation for the pressure in the complex $\hat{\mu}_B$ plane, taking directly subsequent derivatives with respect to $\hat{\mu}_B$ will give good resummed approximants for, e.g., the net-baryon-number density and higher-order cumulants. In Fig. 8, we, thus, also show approximations for n_B/T^3 and χ_2^B obtained by taking the first and second derivatives of the [4, 4] Padé approximant of P/T^4 (green bands). By construction, the poles of these approximants are identical to those of the [4, 4] Padé approximant of P/T^4. As can be seen, these derivatives agree with the corresponding $[n,4]$ approximants up to values of $\hat{\mu}_B$ similar to those where the latter start to differ from the corresponding Taylor series.

Although the radius of convergence for the Taylor series of all higher-order cumulants is determined by that of the pressure series, the currently available eighth-order Taylor series for the pressure clearly does provide a reliable approximation for higher-order cumulants only in a smaller interval of

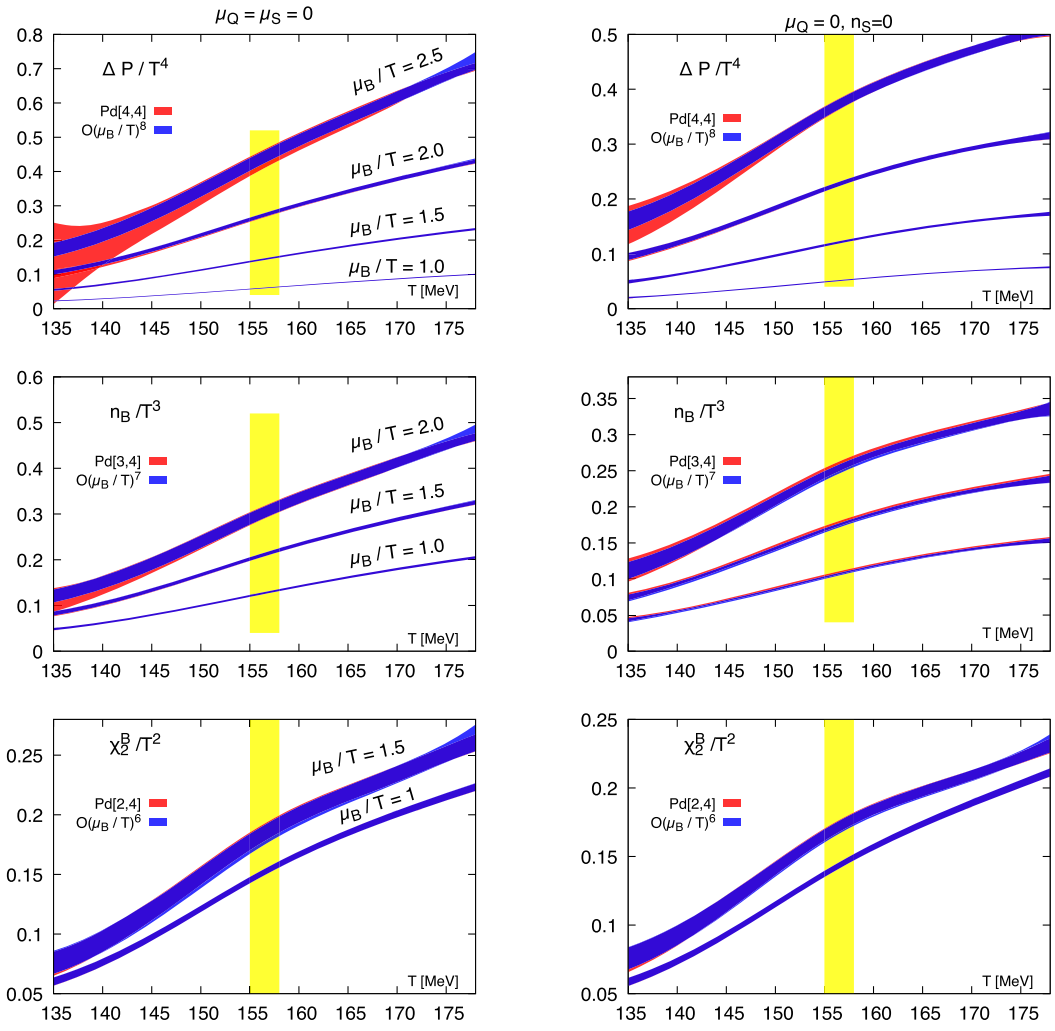

FIG. 9. Comparison of Taylor expansions and $[n,4]$ Padé approximants for the pressure ($n=4$) (top), net-baryon-number density ($n=3$) (middle), and the second-order cumulant ($n=2$) of net-baryon-number fluctuations (bottom) versus temperature for several values of the baryon chemical potential. Shown are results for the cases $\mu_Q=\mu_S=0$ (left) and $\mu_Q=0$, $n_S=0$ (right), respectively. The Taylor expansions are based on the continuum and spline interpolated data shown in Fig. 1.

$\hat{\mu}_B$ values. We consider the range of μ_B values indicated by the range of error bands given in Fig. 8 as the region where current results on the pressure, net-baryon-number density, and the second-order cumulant of net-baryon-number fluctuations are reliable. As can be seen in that figure, this range of baryon chemical potentials is somewhat larger at higher temperatures than at lower temperatures.

In Fig. 9, we compare results obtained for these observables using Taylor expansions as well as Padé approximants for several values of $\hat{\mu}_B$. We show results in the entire temperature range 135 MeV $\leq T \leq$ 175 MeV using values of the chemical potential up to the largest value indicated by the bands given in Fig. 8. As can be seen for the pressure, we find excellent agreement up to values of the chemical potential $\hat{\mu}_B \simeq 2.5$. The corresponding largest values of $\hat{\mu}_B$ for n_B/T^3 and χ_2^B are $\hat{\mu}_B = 2$ and 1.5, respectively. This choice of $\hat{\mu}_B$ values is enforced by demanding good agreement between Taylor series results and Padé approximants at the lowest temperature. At higher temperatures, Figs. 7 and 8 suggest that in the vicinity of T_{pc} the range of $\hat{\mu}_B$ values in which eighth-order Taylor series can provide reliable results is larger, e.g., $\hat{\mu}_B \lesssim 3$ for P/T^4.

V. CONCLUSIONS

We have presented results for eighth-order Taylor series expansions of the pressure in $(2+1)$-flavor QCD for isospin symmetric matter corresponding to vanishing electric charge chemical potentials. From this Taylor series, we derived the first two cumulants of net-baryon-number fluctuations, corresponding to the mean and variance of the net-baryon-number distribution. We used Padé approximants to resum these Taylor series.

We have shown that the [4, 4] Padé approximant, which reproduces the eighth-order Taylor series of the pressure series, has only complex poles in the entire temperature interval 135 MeV $\leq T \leq$ 165 MeV, which gives further support to the observation that a possible critical point in the QCD phase diagram may be found only at temperatures below 135 MeV. From the location of the poles in the complex plane, we estimate the radius of the convergence for these Taylor series expansions to be slightly temperature dependent, increasing from $\hat{\mu}_{B,c} \simeq 2.2$ at $T = 135$ MeV to $\hat{\mu}_{B,c} \simeq 3.2$ at $T = 165$ MeV. In the vicinity of the pseudocritical temperature $T_{pc} \simeq 156.5$ MeV, we find $\mu_B/T \gtrsim 2.9$ at vanishing strangeness chemical potential and somewhat larger values for strangeness neutral matter. If poles of $[n, n]$ Padé approximants continue to lie in the complex $\hat{\mu}_B$ plane, an efficient resummation of the Taylor series of the QCD pressure to even larger values of $\hat{\mu}_B$ will be possible in this temperature range.

A comparison of Taylor series and Padé approximants for the Taylor series of the pressure and the first two cumulants of net-baryon-number fluctuations allows us to estimate the range of $\hat{\mu}_B$ values in which current series expansions give reliable results. For the pressure and the first two cumulants in $(2+1)$-flavor QCD, we deduce that the current eighth-order series for the pressure and its derivatives agree well with the resummed [4, 4] Padé approximants and its derivatives for $\hat{\mu}_B \leq 2.5$ (pressure), 2.0 (net number density), and 1.5 (second-order cumulant).

All data presented in the figures of this paper can be found in [42].

ACKNOWLEDGMENTS

This work was supported by (i) the U.S. Department of Energy, Office of Science, Office of Nuclear Physics through Contract No. DE-SC0012704; (ii) the U.S. Department of Energy, Office of Science, Office of Nuclear Physics and Office of Advanced Scientific Computing Research within the framework of Scientific Discovery through Advance Computing (SciDAC) award *Computing the Properties of Matter with Leadership Computing Resources*; (iii) the Deutsche Forschungsgemeinschaft (DFG, German Research Foundation)—Project No. 315477589-TRR 211; (iv) Grant No. 05P2018 (ErUM-FSP T01) of the German Bundesministerium für Bildung und Forschung; and (v) Grant No. 283286 of the European Union. D. B. was supported by the Intel Corporation. This research used awards of computer time provided by (i) the INCITE program at Oak Ridge Leadership Computing Facility, a DOE Office of Science User Facility operated under Contract No. DE-AC05-00OR22725; (ii) the ALCC program at National Energy Research Scientific Computing Center, a U.S. Department of Energy Office of Science User Facility operated under Contract No. DE-AC02-05CH11231; (iii) the INCITE program at Argonne Leadership Computing Facility, a U.S. Department of Energy Office of Science User Facility operated under Contract No. DE-AC02-06CH11357; and (iv) the USQCD resources at the Thomas Jefferson National Accelerator Facility. This research also used computing resources made available through (i) a PRACE grant at CINECA, Italy; (ii) the Gauss Centre for Supercomputing at the Jülich Supercomputing Centre, Germany; and (iii) the GPU-cluster at Bielefeld University, Germany.

APPENDIX A: TAYLOR EXPANSION COEFFICIENTS FOR STRANGENESS NEUTRAL, ISOSPIN SYMMETRIC QCD MATTER

We give here the general form of the eighth-order expansion coefficients $\bar{\chi}_n^{B,k}$ for nth-order cumulants of net-baryon-number fluctuations. In the context of this work, it is needed only for the pressure series ($n = 0$) in the case $\hat{\mu}_Q = 0$, which corresponds to setting $q_n = 0$ in the following expression. Expansion coefficients of all other cumulants $\bar{\chi}_n^{B,k}$ that involve only cumulants χ_{ijk}^{BQS} with $i + j + k \leq 8$ are given in Appendix A of Ref. [32]:

$$
\begin{aligned}
\bar{\chi}_n^{B,8} = {} & 40320\chi_{n02}^{BQS} s_1 s_7 + 40320\chi_{n02}^{BQS} s_3 s_5 + 6720\chi_{n04}^{BQS} s_1^3 s_5 + 10080\chi_{n04}^{BQS} s_1^2 s_3^2 + 336\chi_{n06}^{BQS} s_1^5 s_3 \\
& + \chi_{n08}^{BQS} s_1^8 + 40320\chi_{n11}^{BQS} q_1 s_7 + 40320\chi_{n11}^{BQS} q_3 s_5 + 40320\chi_{n11}^{BQS} q_5 s_3 + 40320\chi_{n11}^{BQS} q_7 s_1 + 20160\chi_{n13}^{BQS} q_1 s_1^2 s_5 \\
& + 20160\chi_{n13}^{BQS} q_1 s_1 s_3^2 + 20160\chi_{n13}^{BQS} q_3 s_1^2 s_3 + 6720\chi_{n13}^{BQS} q_5 s_1^3 + 1680\chi_{n15}^{BQS} q_1 s_1^4 s_3 + +336\chi_{n15}^{BQS} q_3 s_1^5 + 8\chi_{n17}^{BQS} q_1 s_1^7 \\
& + 40320\chi_{n20}^{BQS} q_1 q_7 + 40320\chi_{n20}^{BQS} q_3 q_5 + 20160\chi_{n22}^{BQS} q_1^2 s_1 s_5 + 10080\chi_{n22}^{BQS} q_1^2 s_3^2 + 40320\chi_{n22}^{BQS} q_1 q_3 s_1 s_3 \\
& + 20160\chi_{n22}^{BQS} q_1 q_5 s_1^2 + 10080\chi_{n22}^{BQS} q_3^2 s_1^2 + 3360\chi_{n24}^{BQS} q_1^2 s_1^3 s_3 + 1680\chi_{n24}^{BQS} q_1 q_3 s_1^4 + 28\chi_{n26}^{BQS} q_1^2 s_1^6 + 6720\chi_{n31}^{BQS} q_1^3 s_5 \\
& + 20160\chi_{n31}^{BQS} q_1^2 q_3 s_3 + 20160\chi_{n31}^{BQS} q_1^2 q_5 s_1 + 20160\chi_{n31}^{BQS} q_1 q_3^2 s_1 + 3360\chi_{n33}^{BQS} q_1^3 s_1^2 s_3 + 3360\chi_{n33}^{BQS} q_1^2 q_3 s_1^3 \\
& + 56\chi_{n35}^{BQS} q_1^3 s_1^5 + 6720\chi_{n40}^{BQS} q_1^3 q_5 + 10080\chi_{n40}^{BQS} q_1^2 q_3^2 + 1680\chi_{n42}^{BQS} q_1^4 s_1 s_3 + 3360\chi_{n42}^{BQS} q_1^3 q_3 s_1^2 + 70\chi_{n44}^{BQS} q_1^4 s_1^4 \\
& + 336\chi_{n51}^{BQS} q_1^5 s_3 + 1680\chi_{n51}^{BQS} q_1^4 q_3 s_1 + 56\chi_{n53}^{BQS} q_1^5 s_1^3 + 336\chi_{n60}^{BQS} q_1^5 q_3 + 28\chi_{n62}^{BQS} q_1^6 s_1^2 + 8\chi_{n71}^{BQS} q_1^7 s_1 \\
& + \chi_{n80}^{BQS} q_1^8 + 40320\chi_{n+101}^{BQS} s_7 + 20160\chi_{n+103}^{BQS} s_1^2 s_5 + 20160\chi_{n+103}^{BQS} s_1 s_3^2 + 1680\chi_{n+105}^{BQS} s_1^4 s_3 + 8\chi_{n+107}^{BQS} s_1^7 \\
& + 40320\chi_{n+110}^{BQS} q_7 + 40320\chi_{n+112}^{BQS} q_1 s_1 s_5 + 20160\chi_{n+112}^{BQS} q_1 s_3^2 + 40320\chi_{n+112}^{BQS} q_3 s_1 s_3 + 20160\chi_{n+112}^{BQS} q_5 s_1^2 \\
& + 6720\chi_{n+114}^{BQS} q_1 s_1^3 s_3 + 1680\chi_{n+114}^{BQS} q_3 s_1^4 + 56\chi_{n+116}^{BQS} q_1 s_1^6 + 20160\chi_{n+121}^{BQS} q_1^2 s_5 + 40320\chi_{n+121}^{BQS} q_1 q_3 s_3 \\
& + 40320\chi_{n+121}^{BQS} q_1 q_5 s_1 + 20160\chi_{n+121}^{BQS} q_3^2 s_1 + 10080\chi_{n+123}^{BQS} q_1^2 s_1^2 s_3 + 6720\chi_{n+123}^{BQS} q_1 q_3 s_1^3 + 168\chi_{n+125}^{BQS} q_1^2 s_1^5 \\
& + 20160\chi_{n+130}^{BQS} q_1^2 q_5 + 20160\chi_{n+130}^{BQS} q_1 q_3^2 + 6720\chi_{n+132}^{BQS} q_1^3 s_1 s_3 + 10080\chi_{n+132}^{BQS} q_1^2 q_3 s_1^2 + 280\chi_{n+134}^{BQS} q_1^3 s_1^4 \\
& + 1680\chi_{141}^{BQS} q_1^4 s_3 + 6720\chi_{141}^{BQS} q_1^3 q_3 s_1 + 280\chi_{n+143}^{BQS} q_1^4 s_1^3 + 1680\chi_{150}^{BQS} q_1^4 q_3 + 168\chi_{152}^{BQS} q_1^5 s_1^2 + 56\chi_{n+161}^{BQS} q_1^6 s_1 \\
& + 8\chi_{n+170}^{BQS} q_1^7 + 20160\chi_{n+202}^{BQS} s_1 s_5 + 10080\chi_{n+202}^{BQS} s_3^2 + 3360\chi_{n+204}^{BQS} s_1^3 s_3 + 28\chi_{n+206}^{BQS} s_1^6 + 20160\chi_{n+211}^{BQS} q_1 s_5 \\
& + 20160\chi_{n+211}^{BQS} q_3 s_3 + 20160\chi_{n+211}^{BQS} q_5 s_1 + 10080\chi_{n+213}^{BQS} q_1 s_1^2 s_3 + 3360\chi_{n+213}^{BQS} q_3 s_1^3 + 168\chi_{n+215}^{BQS} q_1 s_1^5 \\
& + 20160\chi_{n+220}^{BQS} q_1 q_5 + 10080\chi_{n+220}^{BQS} q_3^2 + 10080\chi_{n+222}^{BQS} q_1^2 s_1 s_3 + 10080\chi_{n+222}^{BQS} q_1 q_3 s_1^2 + 420\chi_{n+224}^{BQS} q_1^2 s_1^4 \\
& + 3360\chi_{n+231}^{BQS} q_1^3 s_3 + 10080\chi_{n+231}^{BQS} q_1^2 q_3 s_1 + 560\chi_{n+233}^{BQS} q_1^3 s_1^3 + 3360\chi_{n+240}^{BQS} q_1^3 q_3 + 420\chi_{n+242}^{BQS} q_1^4 s_1^2 + 168\chi_{n+251}^{BQS} q_1^5 s_1 \\
& + 28\chi_{n+260}^{BQS} q_1^6 + 6720\chi_{n+301}^{BQS} s_5 + 3360\chi_{n+303}^{BQS} s_1^2 s_3 + 56\chi_{n+305}^{BQS} s_1^5 + 6720\chi_{n+310}^{BQS} q_5 + 6720\chi_{n+312}^{BQS} q_1 s_1 s_3 \\
& + 3360\chi_{n+312}^{BQS} q_3 s_1^2 + 280\chi_{n+314}^{BQS} q_1 s_1^4 + 3360\chi_{n+321}^{BQS} q_1^2 s_3 + 6720\chi_{n+321}^{BQS} q_1 q_3 s_1 + 560\chi_{n+323}^{BQS} q_1^2 s_1^3 + 3360\chi_{n+330}^{BQS} q_1^2 q_3 \\
& + 560\chi_{n+332}^{BQS} q_1^3 s_1^2 + 280\chi_{n+341}^{BQS} q_1^4 s_1 + 56\chi_{n+350}^{BQS} q_1^5 + 1680\chi_{n+402}^{BQS} s_1 s_3 + 70\chi_{n+404}^{BQS} s_1^4 + 1680\chi_{n+411}^{BQS} q_1 s_3 \\
& + 1680\chi_{n+411}^{BQS} q_3 s_1 + 280\chi_{n+413}^{BQS} q_1 s_1^3 + 1680\chi_{n+420}^{BQS} q_1 q_3 + 420\chi_{n+422}^{BQS} q_1^2 s_1^2 + 280\chi_{n+431}^{BQS} q_1^3 s_1 + 70\chi_{n+440}^{BQS} q_1^4 \\
& + 336\chi_{n+501}^{BQS} s_3 + 56\chi_{n+503}^{BQS} s_1^3 + 336\chi_{n+510}^{BQS} q_3 + 168\chi_{n+512}^{BQS} q_1 s_1^2 + 168\chi_{n+521}^{BQS} q_1^2 s_1 + 56\chi_{n+530}^{BQS} q_1^3 + 28\chi_{n+602}^{BQS} s_1^2 \\
& + 56\chi_{n+611}^{BQS} q_1 s_1 + 28\chi_{n+620}^{BQS} q_1^2 + 8\chi_{n+701}^{BQS} s_1 + 8\chi_{n+710}^{BQS} q_1 + \chi_{n+800}^{BQS}. \qquad \text{(A1)}
\end{aligned}
$$

APPENDIX B: TAYLOR EXPANSION COEFFICIENTS FOR THE $\bar{\chi}_2^B$ IN THE CASE $\mu_Q = 0$, $n_S = 0$

In Fig. 10, we show the expansion coefficients $\bar{\chi}_2^{B,k}$ for the Taylor series of the second-order cumulant of net-baryon-number fluctuations in (2+1)-flavor QCD defined in Eq. (9).

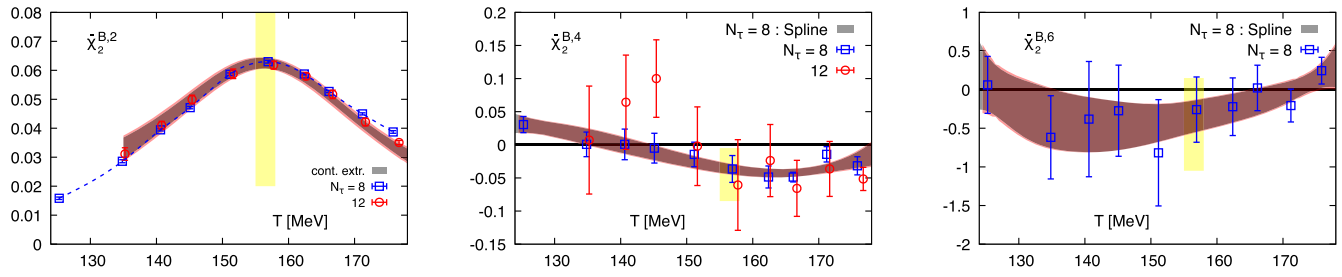

FIG. 10. Taylor expansion coefficients $\bar{\chi}_2^{B,k}$ of the second-order cumulant of net-baryon-number fluctuations in (2 + 1)-flavor QCD.

APPENDIX C: LOCATION OF REAL AND IMAGINARY POLES IN THE PARAMETER SPACE $(c_{6,2}, c_{8,2})$

We discuss here the occurrence of complex and real poles in the plane of the two real expansion parameters appearing in the Taylor series for the pressure, $(c_{6,2}, c_{8,2})$, and characterize the location of [4, 4] Padé approximants constructed from the eighth-order Taylor series of the pressure in $(2+1)$-flavor QCD.

As discussed in Sec. III, there is a triangular-shaped region in this parameter space, bounded by lines $c_{8,2}^{\pm}$ given in Eq. (23), in which all four poles of the [4, 4] Padé are complex with nonvanishing real and imaginary parts. Outside this region, poles of the [4, 4] Padé are either real or purely imaginary. For $z^{\pm} > 0$, there exists a pair of real poles in terms of $\hat{\mu}_B$; for $z^{\pm} < 0$, one has a pair of purely imaginary poles. In the parameter space $(c_{6,2}, c_{8,2})$, one can have two pairs of purely imaginary poles (ii), two pairs of real poles (rr), or a pair of each of these types, (ir) or (ri). In the latter case, we use the convention that the first letter corresponds to that pair of poles that is closest to the origin. The parameters $(c_{6,2}, c_{8,2})$ for which these different types of poles appear are shown in Fig. 11.

In the following, we give some further details on the boundaries for the different regions in parameter space: We rewrite Eq. (22) as

$$z^{\pm} = \frac{c_{8,2} - c_{6,2}}{2(c_{8,2} - c_{6,2}^2)} \pm \frac{\sqrt{(c_{8,2} - c_{6,2})^2 + 4(c_{8,2} - c_{6,2}^2)(1 - c_{6,2})}}{2(c_{8,2} - c_{6,2}^2)}. \quad \text{(C1)}$$

The zeros z^+ and z^- are related to each other through

$$z^+ z^- = \frac{1 - c_{6,2}}{c_{6,2}^2 - c_{8,2}}. \quad \text{(C2)}$$

Outside the region bounded by $c_{8,2}^{\pm}$, both zeros have the same sign, if $z^+ z^- > 0$, i.e., if the numerator and denominator in Eq. (C2) have the same sign, which is the case for

$$\text{either} \quad c_{6,2} > 1 \quad \text{and} \quad c_{8,2} > c_{6,2}^2 \quad \text{(C3)}$$

$$\text{or} \quad c_{6,2} < 1 \quad \text{and} \quad c_{8,2} < c_{6,2}^2. \quad \text{(C4)}$$

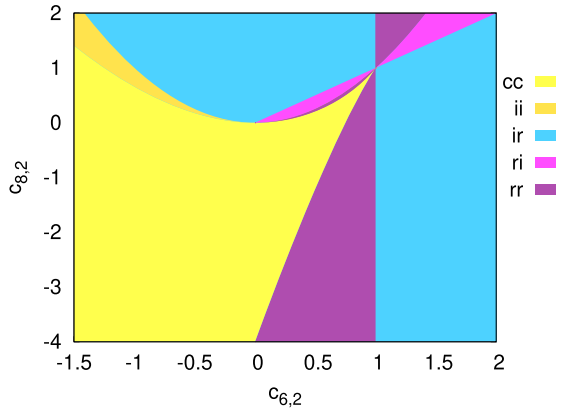

FIG. 11. Location of poles in the complex $\hat{\mu}_B$ plane as a function of the couplings $c_{6,2}$ and $c_{8,2}$. In the yellow area, the four poles are complex (cc) with $\mathrm{Re}\mu_B \neq 0$ and $\mathrm{Im}\mu_B \neq 0$. In the other regions, they come as pairs of two purely real (r) or purely imaginary (i) poles. The notation xy in the legend of the figure indicates that there is a pair of poles of type x and another pair of type y where the poles of type x are closest to the origin.

In the first case, it is obvious that $c_{8,2} > c_{6,2}^2 > c_{6,2}$ holds. It, thus, is evident from Eq. (C1) that $z^+ > 0$ and the region defined in Eq. (C3) corresponds to a region with two real poles in the complex $\hat{\mu}_B$ plane. For all other regions with $c_{6,2} > 1$, a pair of real and a pair of purely imaginary poles exists. However, only for $c_{8,2} < c_{6,2}$ is it the imaginary pair of poles that is closest to the origin.

In the second case [Eq. (C4)], we obtain from Eq. (23)

$$c_{6,2}^2 - c_{8,2}^{+} = (1 - c_{6,2})(2 - c_{6,2} - 2\sqrt{1 - c_{6,2}}) > 0. \quad \text{(C5)}$$

It, thus, is evident from Eq. (C1) that $z^+ < 0$ for $c_{6,2} < 0$. In the range $c_{8,2}^{+} < c_{8,2} < c_{6,2}^2$, one thus finds two pairs of purely imaginary poles in the complex $\hat{\mu}_B$ plane. On the other hand, for $0 < c_{6,2} < 1$, one finds in the same $c_{8,2}$ interval that $z^- > 0$. In this case, one thus has two pairs of real poles in the complex $\hat{\mu}_B$ plane. Finally, there is a second region for purely real poles, which is allowed by Eq. (C4). This is the case of $c_{8,2} < c_{8,2}^{-}$, as also in this case one finds $z^- > 0$. In all other cases, one finds a pair of real and a pair of complex poles. These different parameter regions in the $(c_{6,2}, c_{8,2})$ plane are shown in Fig. 11.

[1] R. V. Gavai and S. Gupta, Phys. Rev. D **71**, 114014 (2005).
[2] C. R. Allton, M. Doring, S. Ejiri, S. J. Hands, O. Kaczmarek, F. Karsch, E. Laermann, and K. Redlich, Phys. Rev. D **71**, 054508 (2005).
[3] M. D'Elia and M.-P. Lombardo, Phys. Rev. D **67**, 014505 (2003).
[4] R. Bellwied, S. Borsanyi, Z. Fodor, J. Günther, S. D. Katz, C. Ratti, and K. K. Szabo, Phys. Lett. B **751**, 559 (2015).
[5] H.-T. Ding, F. Karsch, and S. Mukherjee, Int. J. Mod. Phys. E **24**, 1530007 (2015).
[6] M. D'Elia, Nucl. Phys. **A982**, 99 (2019).
[7] J. N. Guenther, Proc. Sci. LATTICE2021 (2022) 013.
[8] F. Karsch, B.-J. Schaefer, M. Wagner, and J. Wambach, Phys. Lett. B **698**, 256 (2011).
[9] J. N. Guenther, R. Bellwied, S. Borsanyi, Z. Fodor, S. D. Katz, A. Pasztor, C. Ratti, and K. K. Szabó, Nucl. Phys. **A967**, 720 (2017).
[10] C. Bonati, M. D'Elia, F. Negro, F. Sanfilippo, and K. Zambello, Phys. Rev. D **98**, 054510 (2018).
[11] V. Skokov, K. Morita, and B. Friman, Phys. Rev. D **83**, 071502 (2011).
[12] M. A. Stephanov, Phys. Rev. D **73**, 094508 (2006).
[13] M. S. Pradeep and M. Stephanov, Phys. Rev. D **100**, 056003 (2019).
[14] G. Basar, Phys. Rev. Lett. **127**, 171603 (2021).
[15] S. Mukherjee, F. Rennecke, and V. V. Skokov, Phys. Rev. D **105**, 014026 (2022).
[16] M. Wakayama, V. G. Bornyakov, D. L. Boyda, V. A. Goy, H. Iida, A. V. Molochkov, A. Nakamura, and V. I. Zakharov, Phys. Lett. B **793**, 227 (2019).
[17] M. Giordano, K. Kapas, S. D. Katz, D. Nogradi, and A. Pasztor, Phys. Rev. D **101**, 074511 (2020).
[18] S. Mondal, S. Mukherjee, and P. Hegde, Phys. Rev. Lett. **128**, 022001 (2022).
[19] S. Mukherjee and V. Skokov, Phys. Rev. D **103**, L071501 (2021).
[20] G. Nicotra, P. Dimopoulos, L. Dini, F. Di Renzo, J. Goswami, C. Schmidt, S. Singh, K. Zambello, and F. Ziesche, *Proc. Sci.* LATTICE2021 (2022) 260.
[21] P. Dimopoulos, L. Dini, F. Di Renzo, J. Goswami, G. Nicotra, C. Schmidt, S. Singh, K. Zambello, and F. Ziesché, Phys. Rev. D **105**, 034513 (2022).
[22] C. Schmidt, J. Goswami, G. Nicotra, F. Ziesché, P. Dimopoulos, F. Di Renzo, S. Singh, and K. Zambello, Acta Phys. Pol. B Proc. Suppl. **14**, 241 (2021).
[23] H. T. Ding *et al.* (HotQCD Collaboration), Phys. Rev. Lett. **123**, 062002 (2019).
[24] A. M. Halasz, A. D. Jackson, R. E. Shrock, M. A. Stephanov, and J. J. M. Verbaarschot, Phys. Rev. D **58**, 096007 (1998).
[25] R. V. Gavai and S. Gupta, Phys. Rev. D **78**, 114503 (2008).
[26] S. Datta, R. V. Gavai, and S. Gupta, Phys. Rev. D **95**, 054512 (2017).
[27] V. Vovchenko, J. Steinheimer, O. Philipsen, and H. Stoecker, Phys. Rev. D **97**, 114030 (2018).
[28] S. Borsányi, Z. Fodor, J. N. Guenther, R. Kara, S. D. Katz, P. Parotto, A. Pásztor, C. Ratti, and K. K. Szabó, Phys. Rev. Lett. **126**, 232001 (2021).
[29] S. Borsanyi, Z. Fodor, J. N. Guenther, R. Kara, P. Parotto, A. Pasztor, C. Ratti, and K. K. Szabo, arXiv:2202.05574.
[30] G. Basar, G. Dunne, and Z. Yin, arXiv:2112.14269.
[31] A. Bazavov *et al.* (HotQCD Collaboration), Phys. Lett. B **795**, 15 (2019).
[32] A. Bazavov *et al.*, Phys. Rev. D **101**, 074502 (2020).
[33] D. Bollweg, J. Goswami, O. Kaczmarek, F. Karsch, S. Mukherjee, P. Petreczky, C. Schmidt, and P. Scior (HotQCD Collaboration), Phys. Rev. D **104**, 074512 (2021).
[34] E. Follana, Q. Mason, C. Davies, K. Hornbostel, G. Lepage, J. Shigemitsu, H. Trottier, and K. Wong (HPQCD, UKQCD Collaborations), Phys. Rev. D **75**, 054502 (2007).
[35] A. Bazavov *et al.*, Phys. Rev. D **95**, 054504 (2017).
[36] P. M. Lo, B. Friman, M. Marczenko, K. Redlich, and C. Sasaki, Phys. Rev. C **96**, 015207 (2017).
[37] V. Vovchenko, M. I. Gorenstein, and H. Stoecker, Phys. Rev. Lett. **118**, 182301 (2017).
[38] M. A. Clark and A. D. Kennedy, Phys. Rev. Lett. **98**, 051601 (2007).
[39] A. Bazavov *et al.* (MILC Collaboration), Phys. Rev. D **82**, 074501 (2010).
[40] L. Altenkort, D. Bollweg, D. A. Clarke, O. Kaczmarek, L. Mazur, C. Schmidt, P. Scior, and H.-T. Shu, *Proc. Sci.* LATTICE2021 (2022) 196.
[41] G. N. Mercer and A. J. Roberts, SIAM J. Appl. Math. **50**, 1547 (1990).
[42] D. Bollweg, J. Goswami, O. Kaczmarek, F. Karsch, S. Mukherjee, P. Petreczky, C. Schmidt, and P. Scior, 10.4119/unibi/2962427 (2022).